Available online at www.sciencedirect.com
SCIENCE DIRECT®
Automatica 40 (2004) 1677–1687
automatica
www.elsevier.com/locate/automatica

Generating 3-D multi-scroll chaotic attractors: A hysteresis series switching method☆

Jinhu Lü[a], Fengling Han[b], Xinghuo Yu[b,*], Guanrong Chen[c]

[a] *Institute of Systems Science, Academy of Mathematics and Systems Science, Chinese Academy of Sciences, Beijing 100080, China*
[b] *School of Electrical and Computer Engineering, Royal Melbourne Institute of Technology University, Melbourne VIC 3001, Australia*
[c] *Department of Electronic Engineering, City University of Hong Kong, China*

Received 11 May 2003; received in revised form 1 March 2004; accepted 18 May 2004

Abstract

This paper introduces a systematic method—a hysteresis series switching approach—for generating multi-scroll chaotic attractors from a three-dimensional linear autonomous system, including 1-D n-scroll, 2-D $n \times m$-grid scroll, and 3-D $n \times m \times l$-grid scroll chaotic attractors. The chaos generation mechanism is studied by analyzing the system trajectories and the hysteresis switching dynamics of the controlled chaotic systems are explored. Moreover, a two-dimensional Poincaré return map is rigorously derived. This map and its maximum Lyapunov exponent are applied to verifying the chaotic behaviors of the generated 3-D multi-scroll chaotic attractors.
© 2004 Elsevier Ltd. All rights reserved.

Keywords: Chaos generation; Multi-scroll chaotic attractor; Hysteresis series; Switching control

1. Introduction

Over the last two decades, chaos has been found to be useful with great potential in many technological disciplines such as information and computer sciences, biomedical engineering, power systems protection, flow dynamics and liquid mixing, encryption and communications, etc (Chen & Dong, 1998). Recently, there has been some increasing interest in exploiting chaotic dynamics for real-world engineering applications, in which much attention has been focused on effectively generating chaos from simple systems by using simple controllers (Chen & Dong, 1998; Chen, 1999; Lü, Lu, & Chen, 2002a).

Today, generating n-scroll chaotic attractors is no longer a difficult task. Suykens and his colleagues proposed some effective methods for generating n-scroll attractors with simple circuits (Suykens & Vandewalle, 1993; Yalcin, Ozoguz, Suykens, & Vandewalle, 2001; Yalcin, Suykens, Vandewalle, & Ozoguz, 2002). By introducing some additional breakpoints in the piecewise-linear characteristic of the nonlinear resistor of Chua's circuit, they are able to generate not only numerically but also electronically n-double scroll chaotic attractors (Suykens & Vandewalle, 1993). Also, they are able to create a large family of grid-scroll attractors (Yalcin et al., 2002). Kennedy and his colleagues have also constructed a class of circuit-independent chaotic oscillators (Elwakil, Salama, & Kennedy, 2000; Elwakil & Kennedy, 2000, 2001; Ozoguz, Elwakil, & Salama, 2002). Along this line, Tang et al. also designed and simulated some simple sine-function circuits to generate n-scroll chaotic attractors, with circuit realization that can physically produce up to as many as ten scrolls visible on the oscilloscope (Tang, Zhong, Chen, & Man, 2001; Zhong, Man, & Chen, 2002). Lü and his colleagues recently presented a switching piecewise-linear control approach for generating chaotic attractors with multiple-merged basins of attraction (Lü, Zhou, Chen, & Yang, 2002b; Lü, Yu, & Chen, 2003).

It is well known that hysteresis can easily generate chaos (Newcomb & El-Leithy, 1986; Saito, 1990; Saito &

☆ This paper was not presented at any IFAC meeting. This paper was recommended for publication in revised form by Associate Editor Zhihua Qu under the direction of Editor Hassan Khalil.

* Corresponding author. Tel.: +61-3-99254492; fax: +61-3-99254343.
E-mail addresses: jhlu@mail.iss.ac.cn (J. Lü), s3044014@student.rmit.edu.au (F. Han), x.yu@rmit.edu.au (X. Yu), gchen@ee.cityu.edu.hk (G. Chen).

0005-1098/$ - see front matter © 2004 Elsevier Ltd. All rights reserved.
doi:10.1016/j.automatica.2004.06.001

Nakagawa, 1995; Nakagawa & Saito, 1996; Kennedy & Kennedy, 1999; Storace, Parodi, & Robatto, 1999; Kataoka & Saito, 2001; Han, Lü, Yu, Chen, & Feng, 2004). In fact, it was reported that double-scroll chaotic attractors can be generated by a second-order analog circuit consisting of only two capacitors, two resistors, one linear voltage control voltage source (VCVS), and one hysteresis VCVS (Nakagawa & Saito, 1996). Some hysteresis chaotic oscillators were introduced lately (Kennedy & Kennedy, 1999). Chaotic hysteresis circuit realization was reported by Newcomb and El-Leithy (1986), with dynamics and applications being investigated in some details by Storace et al. (1999). Moreover, Saito and his colleagues proposed some higher-dimensional hysteresis chaos generators (Saito, 1990; Saito & Nakagawa, 1995; Kataoka & Saito, 2001). Very recently, we developed a systematic method for generating multi-scroll chaotic attractors in a two-dimensional linear system with hysteresis (Han et al., 2004). These reported results and the need of real-world applications altogether have thus stimulated the present research on generating complex multi-scroll chaotic attractors by using simple systems with only lower-order polynomial nonlinearities.

In this paper, a new systematical method is developed for generating one-directional (1-D) n-scroll, two-directional (2-D) $n \times m$-grid scroll, and three-directional (3-D) $n \times m \times l$-grid scroll chaotic attractors. A two-dimensional Poincaré return map is used to analyze the chaotic behaviors of the multi-scroll chaotic attractors in a three-dimensional systems with hysteresis series. Furthermore, the hysteresis switching dynamics and chaos generation mechanism of the controlled systems are further investigated by a careful analysis of their trajectories. It should be pointed out that the method proposed here is completely different from the method suggested in Yalcin et al. (2002). This is because the basic generator in this paper is the hysteresis function, while the basic generator in Yalcin et al. (2002) is the stair function. Especially, hysteresis function and stair function belong to two different kinds of functions, which have different forming mechanisms.

Note also that there is a substantial difference between the analysis of the 2-D hysteresis system studied by us (Han et al., 2004) and the 3-D hysteresis system studied here, in that the latter presents much complex dynamical behaviors. By proposing the tailored Poincaré map, we are able to give rigorous mathematical proofs for the chaotic behaviors of the 3-D multi-scroll systems. Moreover, our method for verifying the chaotic behaviors of the 3-D multi-scroll systems is completely different from that of the 2-D case used in Han et al. (2004). That is, we prove the chaotic behaviors of the 3-D multi-scroll systems in this paper by constructing a two-dimensional Poincaré return map. However, we verify the chaotic behaviors of the 2-D multi-scroll systems in Han et al. (2004) by analyzing the trajectory distribution. Furthermore, our method here is generic and in principle can be used to deal with k-D ($k \geqslant 3$) multi-scroll systems.

The rest of this paper is organized as follows: In Section 2, a hysteresis series is introduced and some fundamental conditions of chaos generation are discussed for a given three-dimensional linear autonomous system. In Section 3, a new systematic method for generating multi-scroll chaotic attractors, including 1-D n-scroll, 2-D $n \times m$-grid scroll, and 3-D $n \times m \times l$-grid scroll attractors, are presented for a given three-dimensional linear autonomous system with hysteresis series switchings. The hysteresis switching dynamics of the controlled chaotic systems are further analyzed, and a two-dimensional Poincaré return map is rigorously derived for verifying the chaotic behaviors of the multi-scroll systems, in Section 4. Conclusions are finally drawn in Section 5.

2. Preliminaries

This section introduces the hysteresis series concept and gives some fundamental conditions for generating multi-scroll chaotic attractors from a three-dimensional linear autonomous system.

2.1. Hysteresis series

Consider the following hysteresis function:

$$h(x) = \begin{cases} 0 & \text{for } x < 1, \\ 1 & \text{for } x > 0, \end{cases} \tag{1}$$

where $h(x)$ is switched from 1 to 0 if x reaches the threshold 0 from above and is switched from 0 to 1 if x reaches 1 from below, as shown in Fig. 1.

Definition 1. The following function,

$$h(x, p, q) = \sum_{i=1}^{p} h_{-i}(x) + \sum_{i=1}^{q} h_i(x), \tag{2}$$

is called a *hysteresis series*, where p and q are positive integers, and $h_i(x) = h(x - i + 1)$ and $h_{-i}(x) = -h_i(x)$.

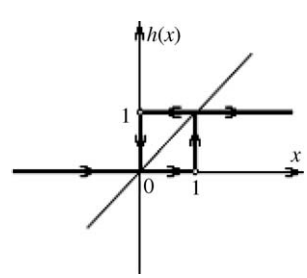

Fig. 1. Hysteresis function.

Note that the hysteresis series $h(x, p, q)$ can be recast as follows:

$$h(x,p,q)=\begin{cases} -p & \text{for } x<-p+1, \\ i & \text{for } \begin{array}{l} i-1<x<i+1, \\ i=-p+1,\ldots,q-1, \end{array} \\ q & \text{for } x>q-1. \end{cases} \tag{3}$$

2.2. Some fundamental conditions for chaos generation

It is well known that chaos is characterized by trajectory boundedness, continuous spectrum, fractional dimensions, strange attractors, etc. In this paper we consider the following two conditions as the main criteria for chaos generation: (i) the trajectories of system are bounded; (ii) there are not any stable ordinary attractors such as stable equilibrium points or stable limit cycles in the bounded region. Other factors will be further considered in the near future. Consider the following three-dimensional linear autonomous system:

$$\begin{pmatrix} \dot{x} \\ \dot{y} \\ \dot{z} \end{pmatrix} = \begin{pmatrix} 0 & 1 & 0 \\ 0 & 0 & 1 \\ -a & -b & -c \end{pmatrix} \begin{pmatrix} x \\ y \\ z \end{pmatrix} \equiv \mathbf{A} \begin{pmatrix} x \\ y \\ z \end{pmatrix}, \tag{4}$$

where x, y, z are state variables, and a, b, c are real constants. To generate chaos from the linear system (4), it needs to design a controller to stretch and fold repeatedly the trajectories of the system. System (4) has a unique equilibrium point $(0,0,0)$ and its corresponding characteristic equation is

$$\lambda^3 + c\lambda^2 + b\lambda + a = 0. \tag{5}$$

Denote $\bar{p} = b - \frac{1}{3}c^2$, $\bar{q} = \frac{2}{27}c^3 - \frac{1}{3}bc + a$, and $\Delta = ac^3/27 - b^2c^2/108 - abc/6 + b^3/27 + a^2/4$. According to the classical formula of the solution of the cubic equations, solving Eq. (5) gives $\lambda_1 = -\frac{c}{3} + \sqrt{-\frac{\bar{q}}{2} + \sqrt{\Delta}} + \sqrt{-\frac{\bar{q}}{2} - \sqrt{\Delta}}$ and $\lambda_{2,3} = -\frac{c}{3} - \frac{1}{2}\left(\sqrt{-\frac{\bar{q}}{2} + \sqrt{\Delta}} + \sqrt{-\frac{\bar{q}}{2} - \sqrt{\Delta}}\right) \pm \frac{\sqrt{3}}{2}\mathrm{i}\left(\sqrt{-\frac{\bar{q}}{2} + \sqrt{\Delta}} - \sqrt{-\frac{\bar{q}}{2} - \sqrt{\Delta}}\right) \equiv \alpha \pm \beta\mathrm{i}$.

Numerical simulations have shown that the linear system (4) can generate chaos by using the hysteresis series switchings under the conditions of $\lambda_1 < 0$, $\alpha > 0$, and $\beta \neq 0$. That is, Eq. (5) has a negative eigenvalue and a pair of complex conjugately eigenvalues with positive real parts. Moreover, the equilibrium point $(0,0,0)$ is a two-dimensionally unstable saddle point. Therefore, one may assume that

$$\Delta = \frac{ac^3}{27} - \frac{b^2c^2}{108} - \frac{abc}{6} + \frac{b^3}{27} + \frac{a^2}{4} > 0,$$

$$\lambda_1 = -\frac{c}{3} + \sqrt{-\frac{\bar{q}}{2} + \sqrt{\Delta}} + \sqrt{-\frac{\bar{q}}{2} - \sqrt{\Delta}} < 0,$$

$$\alpha = -\frac{c}{3} - \frac{1}{2}\left(\sqrt{-\frac{\bar{q}}{2} + \sqrt{\Delta}} + \sqrt{-\frac{\bar{q}}{2} - \sqrt{\Delta}}\right) > 0. \tag{6}$$

In the following, we present a systematic method for generating multi-scroll chaotic attractors via hysteresis series switchings in the linear autonomous system (4).

3. Generating multi-scroll chaotic attractors

This section presents a new systematic method—hysteresis series switching approach—for generating multi-scroll chaotic attractors, including 1-D n-scroll, 2-D $n \times m$-grid scroll, and 3-D $n \times m \times l$-grid scroll, in the linear system (4). Consider a unified hybrid system, which can be regarded as a linear system with a hysteresis series feedback nonlinearity and is described by

$$\dot{X} = \mathbf{A}X + \mathbf{B}\theta(X), \tag{7}$$

where $X = (x, y, z)^{\mathrm{T}}$ is the state vector, and $\mathbf{A}$ is defined in (4) and $\mathbf{B} = -\mathbf{A}$. Here, one has three different cases as follows.

3.1. Generating n-scroll chaotic attractors

In the following, a hysteresis series controller is added to system (4), aiming to generate n-scroll chaotic attractors. Assume that

$$\theta(X) = \begin{pmatrix} h(x, p_1, q_1) \\ 0 \\ 0 \end{pmatrix}, \tag{8}$$

where $u = h(x, p_1, q_1)$ is defined by (3). Obviously, the equilibrium points of system (7) with controller (8) are all located along the x-axis, given by

$$O_x = [-p_1, -p_1 + 1, \ldots, 0, \ldots, q_1 - 1, q_1]. \tag{9}$$

Thus, system (7) with controller (8) has the potential to create a $(p_1 + q_1 + 1)$-scroll chaotic attractor for some suitable parameters a, b, c. Fig. 2 shows a 7-scroll chaotic attractor

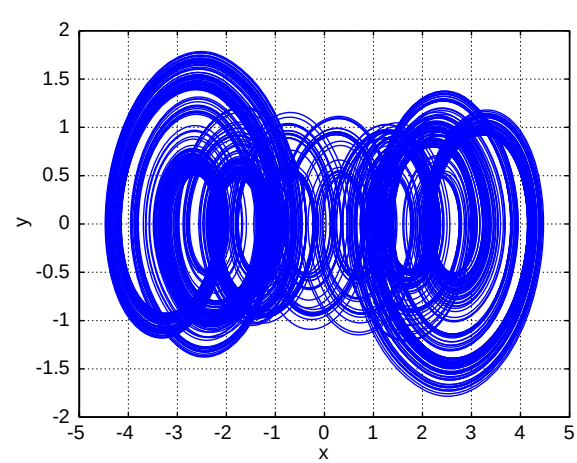

Fig. 2. A 1-D 7-scroll chaotic attractor.

of system (7) with controller (8), where $a = 0.8$, $b = 0.72$, $c = 0.6$, $p_1 = q_1 = 3$.

It is noticed that system (7) with controller (8) is a four-dimensional system of (x, y, z, u) and can be regarded as a configuration of $(p_1 + q_1 + 1)$ three-dimensional linear systems on $(p_1 + q_1 + 1)$ subspaces connected one another via switchings by the hysteresis series $h(x, p_1, q_1)$. Denote

$$S_{-r_1}(\xi) = \{\xi | \xi < -r_1 + 1\},$$

$$S_i(\xi) = \{\xi | i - 1 < \xi < i + 1\} \quad \text{for} \quad -r_1 + 1 \leqslant i \leqslant r_2 - 1,$$

$$S_{r_2}(\xi) = \{\xi | \xi > r_2 - 1\}. \tag{10}$$

When $\xi = x$, $r_1 = p_1$, and $r_2 = q_1$, denote $S_i(x) = S_i$ for $-p_1 \leqslant i \leqslant q_1$. The subspaces are $V_i = \{\bar{X} | x \in S_i,\ u = i\}$, where $-p_1 \leqslant i \leqslant q_1$ and $\bar{X} = (x, y, z, u)$. It is clear that there exists one and only one equilibrium point in every subspace $V_i(-p_1 \leqslant i \leqslant q_1)$. Moreover, system (7) with controller (8) is unstable in each subspace V_i, thus the system trajectories will not stay in any subspace forever.

For a given initial value $(x_0, y_0, z_0, u_0) \in V_i$, as $t \to +\infty$, the trajectory of system (7) with controller (8) spirally diverges around its equilibrium point in subspace V_i; when the trajectory reaches the boundaries of subspace V_i, it jumps onto another neighboring subspace V_j $(j \neq i)$ holding (x, y, z) constant, and then continuously to do so. Here, the switching boundaries are planes rather than lines for the two-dimensional case. Note that the trajectory will go through every subspace $V_j(-p_1 \leqslant j \leqslant q_1)$. After a long enough time, the trajectory definitely returns to the original subspace V_i, and then repeats similar motion for infinitely many times. As $t \to +\infty$, the system changes its dynamical behaviors (folding and stretching dynamics) repeatedly as the trajectory goes through the $(p_1 + q_1 + 1)$ regions alternately and repeatedly. It should be emphasized that the switching planes of the hysteresis series $h(x, p_1, q_1)$ play a key role in creating chaos. Also, it is clear that the switching mechanics of the controlled system (7) with controller (8) are more complex than that of the two-dimensional case.

3.2. Generating 2-D $n \times m$-grid scroll chaotic attractors

In this subsection, a hysteresis series controller is added to system (4) for creating 2-D $n \times m$-grid scroll chaotic attractors. Suppose that

$$\theta(X) = \begin{pmatrix} h(x, p_1, q_1) \\ h(y, p_2, q_2) \\ 0 \end{pmatrix}, \tag{11}$$

where $u = h(x, p_1, q_1)$ and $v = h(y, p_2, q_2)$, both are defined by (3). Obviously, system (7) with controller (11) has $(p_1 + q_1 + 1) \times (p_2 + q_2 + 1)$ equilibrium points located in the x–y plane, given by

$$O_{xy} = \{(i, j) | -p_1 \leqslant i \leqslant q_1, -p_2 \leqslant j \leqslant q_2\}. \tag{12}$$

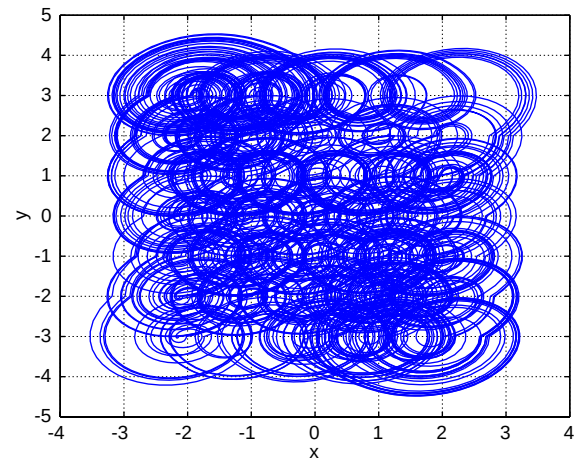

Fig. 3. A 2-D 5×7-grid scroll chaotic attractor.

Thus, for some suitable parameters a, b, c, system (7) with controller (11) can create a $(p_1+q_1+1)\times(p_2+q_2+1)$-scroll chaotic attractor, called 2-D $n \times m$-*grid scroll* chaotic attractor. Fig. 3 shows a 5×7-grid scroll chaotic attractor, where $a = 0.8$, $b = 0.7$, $c = 0.6$, $p_1 = q_1 = 2$, $p_2 = q_2 = 3$. It is clear that there are 5 scrolls in the x-direction and 7 scrolls in the y-direction, as shown in Fig. 3.

Note that system (7) with controller (11) is a five-dimensional system of (x, y, z, u, v) and can be regarded as a configuration of $(p_1 + q_1 + 1) \times (p_2 + q_2 + 1)$ 3-D linear systems on $(p_1 + q_1 + 1) \times (p_2 + q_2 + 1)$ subspaces connected one another via the switchings by the hysteresis series $h(x, p_1, q_1)$ and $h(y, p_2, q_2)$. From (10), when $\xi = y$, $r_1 = p_2$, and $r_2 = q_2$, denote $S_j(y) = T_j$ for $-q_2 \leqslant j \leqslant q_2$. Thus, the subspaces are

$$V_{(i,j)} = \{\bar{X} | x \in S_i,\ y \in T_j,\ u = i,\ v = j\}, \tag{13}$$

where $-p_1 \leqslant i \leqslant q_1$, $-p_2 \leqslant j \leqslant q_2$, and $\bar{X} = (x, y, z, u, v)$.

It is clear that there exists one and only one equilibrium point in each subspace $V_{(i,j)}(-p_1 \leqslant i \leqslant q_1;\ -p_2 \leqslant j \leqslant q_2)$. Moreover, the system trajectories will not stay in any subspace forever since system (7) with controller (11) is unstable in every subspace $V_{(i,j)}$. Note that those 2-D $n \times m$-grid scroll chaotic attractors are generated in exactly the same way as the 1-D case discussed in the last subsection, except the directions of the system trajectories are more vertical here. Similarly, one can design the 2-D $n \times m$-grid scroll attractors in x–z or y–z direction.

3.3. Generating 3-D $n \times m \times l$-grid scroll chaotic attractors

In the following, a hysteresis series controller is added to system (4) for generating 3-D $n \times m \times l$-grid scroll chaotic attractors. Assume that

$$\theta(X) = \begin{pmatrix} h(x, p_1, q_1) \\ h(y, p_2, q_2) \\ h(z, p_3, q_3) \end{pmatrix}, \tag{14}$$

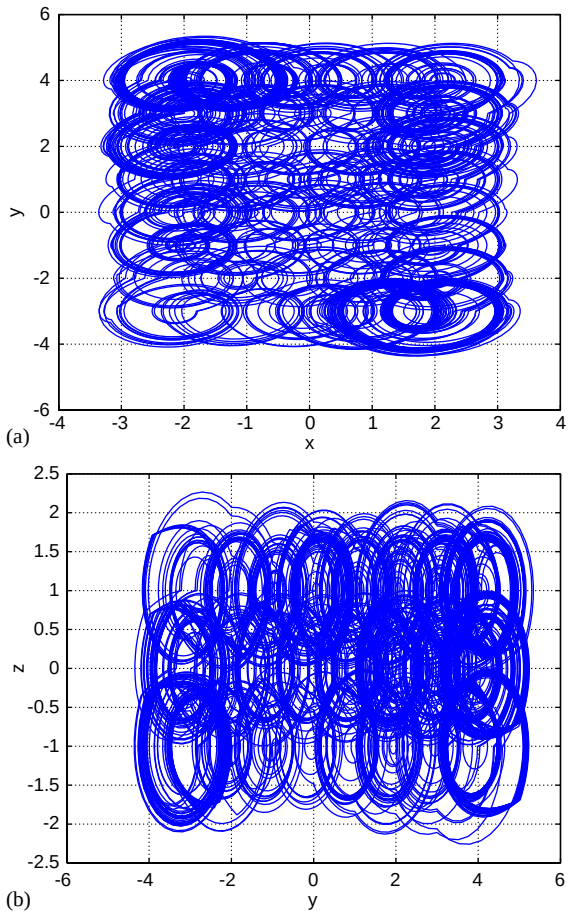

Fig. 4. A 3-D $5 \times 8 \times 3$-grid scroll chaotic attractors: (a) x–y plane; and (b) y–z plane.

where $u = h(x, p_1, q_1)$, $v = h(y, p_2, q_2)$, and $w = h(z, p_3, q_3)$ are all defined by (3). Clearly, system (7) with controller (14) has $(p_1 + q_1 + 1) \times (p_2 + q_2 + 1) \times (p_3 + q_3 + 1)$ equilibrium points, which are given by

$$O_{xyz} = \{(i, j, k) | -p_1 \leqslant i \leqslant q_1, -p_2 \leqslant j \leqslant q_2, -p_3 \leqslant k \leqslant q_3\}. \tag{15}$$

Therefore, for some suitable parameters a, b, c, system (7) with controller (14) can generate a $(p_1 + q_1 + 1) \times (p_2 + q_2 + 1) \times (p_3 + q_3 + 1)$-scroll chaotic attractor, called 3-D $n \times m \times l$-*grid scroll* chaotic attractor. Fig. 4 shows a $5 \times 8 \times 3$-grid scroll chaotic attractor, where $a = 0.8$, $b = 0.72$, $c = 0.66$, $p_1 = q_1 = 2$, $p_2 = 3$, $q_2 = 4$, $p_3 = q_3 = 1$. It is clear that there are 5 scrolls in the x-direction, 8 scrolls in the y-direction, and 3 scrolls in the z-direction, as shown in Fig. 4.

It is noticed that system (7) with controller (14) is a six-dimensional system of (x, y, z, u, v, w) and can be regarded as a configuration of $(p_1 + q_1 + 1) \times (p_2 + q_2 + 1) \times (p_3 + q_3 + 1)$ 3-D linear systems on $(p_1 + q_1 + 1) \times (p_2 + q_2 + 1) \times (p_3 + q_3 + 1)$ subspaces connected one another via the switchings by the hysteresis series $h(x, p_1, q_1)$, $h(y, p_2, q_2)$, and $h(z, p_3, q_3)$. According to (10), when $\xi = z$, $r_1 = p_3$, and $r_2 = q_3$, denote $S_k(z) = U_k$ for $-p_3 \leqslant k \leqslant q_3$. Then the subspaces are

$$V_{(i,j,k)} = \{\bar{X} | x \in S_i,\ y \in T_j,\ z \in U_k, u = i, v = j,\ w = k\}, \tag{16}$$

where $-p_1 \leqslant i \leqslant q_1$, $-p_2 \leqslant j \leqslant q_2$, $-p_3 \leqslant k \leqslant q_3$, and $\bar{X} = (x, y, z, u, v, w)$.

There exists one and only one equilibrium point in each subspace $V_{(i,j,k)}(-p_1 \leqslant i \leqslant q_1;\ -p_2 \leqslant j \leqslant q_2;\ -p_3 \leqslant k \leqslant q_3)$. Moreover, the system trajectories will not stay in any subspace forever since system (7) with controller (14) is unstable in every subspace $V_{(i,j,k)}$. These 3-D $n \times m \times l$-grid scroll chaotic attractors are generated in exactly the same way as 1-D and 2-D cases studied before.

Note that parameters $p_i, q_i (1 \leqslant i \leqslant 3)$ determine the numbers of the scrolls in the x, y, z-directions, and the hysteresis series $h(x, p_1, q_1)$, $h(y, p_2, q_2)$, and $h(z, p_3, q_3)$ determine the positions of the scrolls. Moreover, one can arbitrarily design the number and also the position of the scrolls of the hysteresis controlled chaotic system (7). One can also rotate the multi-scroll hysteresis chaotic attractors to any desired orientation in the state space. Note that every subspace has one and only one equilibrium point, and every equilibrium point corresponds to one scroll of the chaotic attractor of the hysteresis controlled system (7). The trajectories of system (7) are repeatedly stretched and folded in the state space for infinitely many times via hysteresis switchings, leading to the appearance of bifurcations and chaos. Clearly, the dynamical behaviors of each piece of the system are rather simple and it has an exact analytic solution in every subspace. However, the dynamical behaviors of the entire system become rather complex because of the hysteresis switchings between subspaces.

Remark 1. In fact, $\theta(X)$ in system (7) is a piecewise constant function and $\dot{\theta} = 0$ in every piecewise region. Moreover, the measure of the set for all switching points is zero. Assume that $Y = X - \mathbf{A}^{-1}\mathbf{B}\theta$, then system (7) becomes system (4). That is, in every subregion, system (7) has the same dynamical behaviors. In essence, the system (7) assembles the dynamical behaviors of system (4) with different initial values in different subregion. It is easy to understand that system (7) has one scroll and one equilibrium point in every subregion.

4. Hysteresis switching dynamics and Poincaré return map

In this section, the switching dynamics of the hysteresis controlled chaotic system (7) with controllers (8), (11), and (14) are further investigated. Especially, a two-dimensional Poincaré return map is rigorously derived for verifying the chaotic behaviors of system (7) with controller (8). Assume

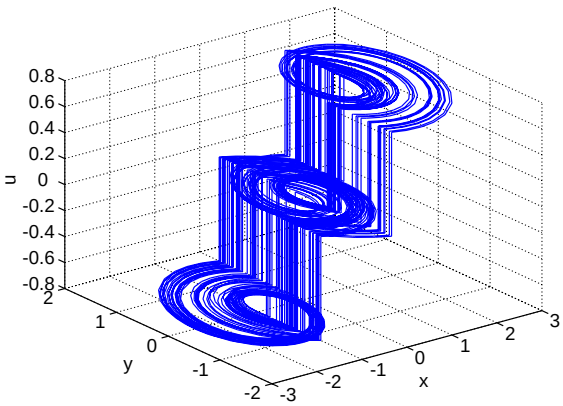

Fig. 5. x–y–u space projection for 1-D 3-scroll hysteresis chaotic attractor.

that (6) holds, so as to guarantee that system (4) has a negative eigenvalue and a pair of conjugate complex eigenvalues with positive real parts.

4.1. Hysteresis switching dynamics of system (7) with controller (8)

Suppose that $a, b, c > 0$ and $p_1 = q_1 = 1$. Then system (7) with controller (8) has a 3-scroll chaotic attractor as shown in Fig. 5. Clearly, it has three equilibria, located in three corresponding subspaces: $(1,0,0,1) \in V_1$, $(0,0,0,0) \in V_0$, $(-1,0,0,-1) \in V_{-1}$, where V_1, V_0, V_{-1} are defined in Section 3.1. Note that system (7) with controller (8) has a natural symmetry under the coordinates transform $(x,y,z) \to (-x,-y,-z)$, which persists for all values of the system parameters.

The variation of the volume $V(t)$ of a small element, $\delta V(t) = \delta x \delta y \delta z$, in the state space is determined by the divergence of the flow: $\nabla V = \partial\dot{x}/\partial x + \partial\dot{y}/\partial y + \partial\dot{z}/\partial z = -c < 0$. Therefore, system (7) with controller (8) is dissipative in each subspace.

On each subspace V_i $(-1 \leqslant i \leqslant 1)$, which are defined in Section 3.1, the dynamical equation is described by

$$(\dot{\bar{x}}, \dot{\bar{y}}, \dot{\bar{z}})^{\mathrm{T}} = \mathbf{A}(\bar{x}, \bar{y}, \bar{z})^{\mathrm{T}}, \tag{17}$$

where

$$(\bar{x}, \bar{y}, \bar{z})^{\mathrm{T}} = (x-1, y, z)^{\mathrm{T}} \quad \text{for } \bar{X} \in V_1,$$

$$(\bar{x}, \bar{y}, \bar{z})^{\mathrm{T}} = (x, y, z)^{\mathrm{T}} \quad \text{for } \bar{X} \in V_0,$$

$$(\bar{x}, \bar{y}, \bar{z})^{\mathrm{T}} = (x+1, y, z)^{\mathrm{T}} \quad \text{for } \bar{X} \in V_{-1},$$

in which $\bar{X} = (x, y, z, u)$. Thus, the exact solution of Eq. (17) is

$$\bar{x}(t) = A_1 \mathrm{e}^{\lambda_1 t} + \mathrm{e}^{\alpha t}(A_2 \cos(\beta t) + A_3 \sin(\beta t)),$$

$$\bar{y}(t) = A_1 \lambda_1 \mathrm{e}^{\lambda_1 t} + \mathrm{e}^{\alpha t}[(A_2\alpha + A_3\beta)\cos(\beta t) + (A_3\alpha - A_2\beta)\sin(\beta t)],$$

$$\bar{z}(t) = A_1 \lambda_1^2 \mathrm{e}^{\lambda_1 t} + \mathrm{e}^{\alpha t}[(A_2\alpha^2 + 2A_3\alpha\beta - A_2\beta^2)\cos(\beta t) + (A_3\alpha^2 - 2A_2\alpha\beta - A_3\beta^2)\sin(\beta t)], \tag{18}$$

where

$$A_1 = \frac{(\alpha^2+\beta^2)\bar{x}(0) - 2\alpha\bar{y}(0) + \bar{z}(0)}{(\lambda_1-\alpha)^2+\beta^2},$$

$$A_2 = \frac{(\lambda_1^2 - 2\alpha\lambda_1)\bar{x}(0) + 2\alpha\bar{y}(0) - \bar{z}(0)}{(\lambda_1-\alpha)^2+\beta^2},$$

$$A_3 = \frac{B_1\bar{x}(0) - (\beta^2-\alpha^2+\lambda_1^2)\bar{y}(0) + (\alpha-\lambda_1)\bar{z}(0)}{\beta\left[(\lambda_1-\alpha)^2+\beta^2\right]},$$

in which $B_1 = \lambda_1\alpha^2 - \lambda_1\beta^2 - \lambda_1^2\alpha$, and λ_1, α, β are given in Section 2.2.

Obviously, system (7) with controller (8) has four hysteresis switching planes:

$$M_1 \equiv \{(x,y,z,u) | x = 0\} \cap V_1,$$

$$M_2 \equiv \{(x,y,z,u) | x = 1\} \cap V_0,$$

$$M_3 \equiv \{(x,y,z,u) | x = -1\} \cap V_0,$$

$$M_4 \equiv \{(x,y,z,u) | x = 0\} \cap V_{-1}$$

and the corresponding switching rules are as follows: (i) $\bar{X}(t^+) = (0,y,z,0) \in V_0$ if $\bar{X}(t) = (0,y,z,1) \in M_1$; (ii) $\bar{X}(t^+) = (1,y,z,1) \in V_1$ if $\bar{X}(t) = (1,y,z,0) \in M_2$; (iii) $\bar{X}(t^+) = (-1,y,z,-1) \in V_{-1}$ if $\bar{X}(t) = (-1,y,z,0) \in M_3$; (iv) $\bar{X}(t^+) = (0,y,z,0) \in V_0$ if $\bar{X}(t) = (0,y,z,-1) \in M_4$, where $\bar{X} = (x,y,z,u)$.

Now, define four specially grazing surfaces (See Fig. 6):

(i) $\overrightarrow{A_1B_1C_1D_1}$ is a trajectory in V_1 that starts from $A_1(0,0,a_1,1) \in M_1$ at $t = 0$, intersects $B_1(1,b_1,\bar{b}_1,1) \in \{\bar{X} | x=1, y<0\} \in V_1$ at $t=t_1$ and $C_1(1,c_1,\bar{c}_1,1) \in \{\bar{X} | x=1, y>0\} \in V_1$ at $t = t_2$, and finally reaches $D_1(0,d_1,\bar{d}_1,1) \in M_1$ at $t = t_3$. Since the starting point A_1 lies in the line $\dot{x} = y = 0$, the trajectory $\overrightarrow{A_1B_1C_1D_1}$ grazes M_1 at A_1. Denote $S_1 = \{\overrightarrow{A_1B_1C_1D_1} | a_1 \in \mathbf{R}\}$. Obviously, surface S_1 grazes the switching plane M_1 at z-axis.

(ii) $\overrightarrow{A_2B_2C_2}$ is a trajectory in V_0 that starts from $A_2(-1,0,a_2,0) \in M_3$ at $t=0$, intersects $B_2(0,b_2,\bar{b}_2,0) \in \{\bar{X} | x = 0, y<0\} \in V_0$ at $t = t_4$ and reaches $C_2(1,c_2,\bar{c}_2,0) \in M_2$ at $t = t_5$. The trajectory $\overrightarrow{A_2B_2C_2}$ grazes M_3 at A_2 since the starting point A_2 lies in the line $\dot{x} = y = 0$. Denote $S_2 = \{\overrightarrow{A_2B_2C_2} | a_2 \in \mathbf{R}\}$. Clearly, surface S_2 grazes the switching plane M_3 at line $M_3 \cap \{y = 0\}$.

(iii) $\overrightarrow{A_2'B_2'C_2'}$ is a trajectory in V_0 that starts from $A_2'(1,0,a_2',0) \in M_2$ at $t = 0$, intersects $B_2'(0,b_2',\bar{b}_2',0) \in \{\bar{X} | x = 0, y>0\} \in V_0$ at $t = t_6$ and reaches $C_2'(-1,c_2',\bar{c}_2',0) \in M_3$ at $t = t_7$. The trajectory $\overrightarrow{A_2'B_2'C_2'}$ grazes M_2 at A_2' since the starting point A_2' lies in the line $\dot{x}=y=0$. Denote $S_2' = \{\overrightarrow{A_2'B_2'C_2'} | a_2' \in \mathbf{R}\}$. Obviously,

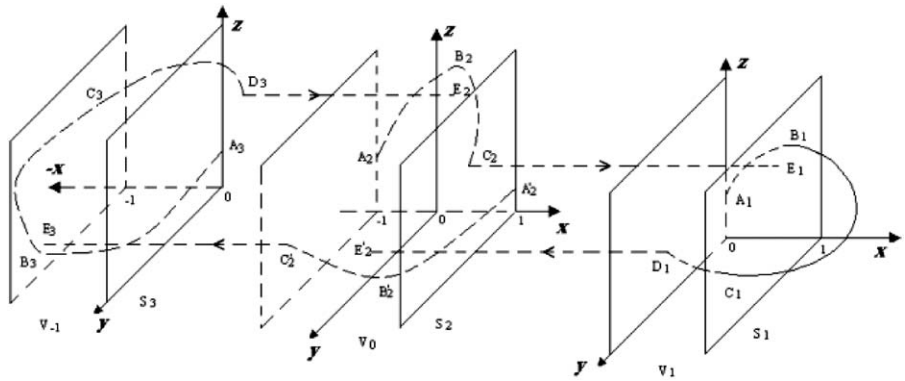

Fig. 6. Trajectories switching of the hysteresis controlled system (7) with controller (8).

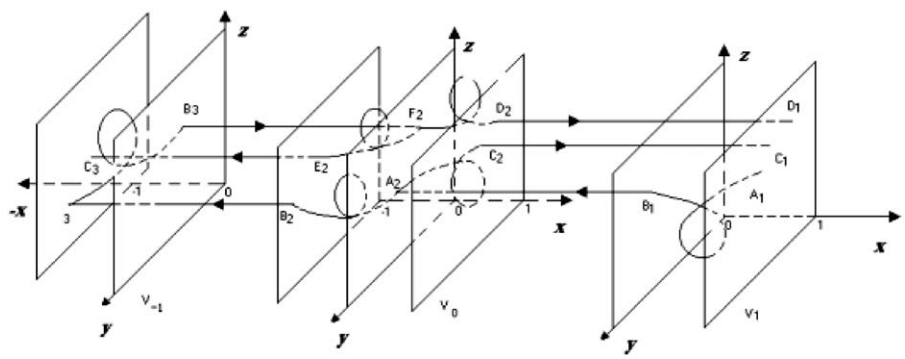

Fig. 7. Hysteresis phase space.

surface S_2' grazes the switching plane M_2 at line $M_2 \cap \{y=0\}$.

(iv) $\overrightarrow{A_3B_3C_3D_3}$ is a trajectory in V_{-1} that starts from $A_3(0,0,a_3,-1) \in M_4$ at $t=0$, intersects $B_3(-1,b_3,\bar{b}_3,-1) \in \{\bar{X}|x=-1, y>0\} \in V_{-1}$ at $t=t_8$ and $C_3(-1,c_3,\bar{c}_3,-1) \in \{\bar{X}|x=-1, y<0\} \in V_{-1}$ at $t=t_9$, and finally reaches $D_3(0,d_3,\bar{d}_3,-1) \in M_3$ at $t=t_{10}$. Note that the starting point A_3 lies in the line $\dot{x}=y=0$, then the trajectory $\overrightarrow{A_3B_3C_3D_3}$ grazes M_3 at A_3. Denote $S_3 = \{\overrightarrow{A_3B_3C_3D_3}|a_3 \in \mathbf{R}\}$. Obviously, surface S_3 grazes the switching plane M_3 at z-axis.

Based on the above four grazing surfaces and the four switching planes, define a special region of trajectories by

$$\Gamma = \Gamma_1 \cup \Gamma_2 \cup \Gamma_3,$$

where Γ_1 is a region in V_1 surrounded by S_1 and M_1, Γ_2 is a region in V_0 surrounded by S_2, S_2', M_2 and M_3, and Γ_3 is a region in V_{-1} surrounded by S_3 and M_4.

Note that all parameters $b_i, \bar{b}_i, c_i, \bar{c}_i$ $(1 \leqslant i \leqslant 3)$, $d_i, \bar{d}_i$ $(i=1,3)$, and $b_2', \bar{b}_2', c_2', \bar{c}_2'$ can be regarded as functions of a,b,c for the given initial points A_1, A_2, A_2', A_3, and can be precisely calculated by using the exact solution (18) and the arriving time t_i $(1 \leqslant i \leqslant 10)$. Moreover, B_1 and B_3, C_1 and C_3, D_1 and D_3, B_2 and B_2', C_2 and C_2' are symmetrical. Denote

$$P_1 = \{(b_1,\bar{b}_1)|a_1 \in \mathbf{R}\},\ N_1 = \{(c_1,\bar{c}_1)|a_1 \in \mathbf{R}\},$$

$$P_2 = \{(b_2,\bar{b}_2)|a_2 \in \mathbf{R}\},\ N_2 = \{(b_2',\bar{b}_2')|a_2' \in \mathbf{R}\},$$

$$P_3 = \{(b_3,\bar{b}_3)|a_3 \in \mathbf{R}\},\ N_3 = \{(c_3,\bar{c}_3)|a_3 \in \mathbf{R}\}$$

and T_1 is a region in $V_1 \cap \{x=1\}$ surrounded by P_1 and N_1, T_2 is a region in $V_0 \cap \{x=0\}$ surrounded by P_2 and N_2, T_3 is a region in $V_{-1} \cap \{x=-1\}$ surrounded by P_3 and N_4.

It is noticed that regions T_1 and T_3 are symmetrical. According to the switching rules and the exact analytic solution (18), one has the following conclusion: Γ is an invariant set if the parameters a,b,c of system (7) with controller (8) satisfy

$$(0, d_1(a,b,c,a_1), \bar{d}_1(a,b,c,a_1), 0) \in T_2$$

and

$$(1, c_2(a,b,c,a_2), \bar{c}_2(a,b,c,a_2), 1) \in T_1,$$

where $a_1 \in \mathbf{R}$ and $a_2 \in \mathbf{R}$. In fact, all trajectories started from any point in Γ will remain in Γ as shown in Fig. 6. That is, Γ is an invariant set. Although the switching rules are very simple, the generated trajectories are rather complex.

In the following, a two-dimensional Poincaré return map is rigorously derived for verifying the chaotic behaviors of the 3-scroll attractor shown in Fig. 7.

Consider a trajectory started from a point $(0, y_0, z_0, 0) \in V_0$ at $t=0$. According to the solution (18), if there are not switchings in the boundaries M_2 and M_3, it must reach M_2 and M_3 at the positive times t_a and t_b separately. Here, t_a

and t_b are the first arriving time. Let $(1, y_1, z_1, 0) \in M_2$ be the hit point. Then one can get the arriving time t_a, y_1 and z_1 by using the exact solution (18). Similarly, for the hit point $(1, y_1', z_1', 0) \in M_3$, one can get the arriving time t_b, y_1' and z_1'. In the following, first define a region by

$$H_0 = \{(0, y, z, 0) \in V_0 \mid t_a < t_b\}. \tag{19}$$

Also, consider a trajectory started from a point $(1, y_0, z_0, 1) \in V_1$ at $t = 0$. Due to (18), it must reach M_1 at some positive time t_c. Let $(0, \bar{y}_1, \bar{z}_1, 1) \in M_1$ be the hit point. Then one can get the arriving time t_c, $\bar{y}_1$ and $\bar{z}_1$, by using the exact solution (18). Thus, define the following region:

$$H_1 = \{(1, y, z, 1) \in V_1 \mid (0, \bar{y}_1, \bar{z}_1, 0) \in H_0\}. \tag{20}$$

Now, consider the vector field in V_1. Let E^{r} be the eigenspace corresponding to the real eigenvalue λ_1 and let E^{c} be the eigenspace corresponding to the complex eigenvalues $\alpha \pm \beta \mathrm{i}$. They are described by $E^{\mathrm{r}} = \{(x, y, z) | \lambda_1^2(x-1) = \lambda_1 y = z, x > 0\}$, $E^{\mathrm{c}} = \{(x, y, z) | (\alpha^2 + \beta^2)(x-1) - 2\alpha y + z = 0, x > 0\}$.

Denote $\Omega_1 = V_1 \cap \{x = 1\}$, $\Omega_2 = V_0 \cap \{x = 0\}$, $\Omega_3 = V_{-1} \cap \{x = -1\}$. Consider a trajectory started from an initial point $(1, y_0, z_0, 1) \in H_1$ at $t = 0$. According to (18), it must reach the switching plane M_1 at some positive time t_1, as shown in Fig. 7. In fact, since $\lambda_1 < 0$, the trajectory will tend to eigenspace E^{c} and spirally diverge at the eigenspace E^{r} with a positive exponential rate $\mathrm{e}^{\alpha t}$. Let $(0, y_1, z_1, 1)$ be the hit point. From the switching rule and (20), the trajectory jumps onto $H_0 \subset \Omega_2$ holding y_1, z_1 constant. That is, the hit point is $(0, y_1, z_1, 0) \in H_0$. Then, according to (19) and (20), the trajectory must reach the switching plane M_2 at some positive time t_2, as displayed in Fig. 7. Let $(1, y_2, z_2, 0)$ be the hit point. From the switching rule, this trajectory jumps onto Ω_1 holding y_2, z_2 constant. Thus, the hit point is $(0, y_2, z_2, 0) \in \Omega_1$.

On the other hand, consider a trajectory started from a point $(1, y_0, z_0, 1) \in \Omega_1 - H_1$ at $t = 0$. According to (18), it must reach the switching plane M_1 at some positive time t_1. Let $(0, y_1, z_1, 1)$ be the hit point. According to the switching rule and (20), this trajectory jumps onto $\Omega_2 - H_0$ holding y_1, z_1 constant. That is, the hit point is $(0, y_1, z_1, 0) \in \Omega_2 - H_0$. Due to (19), the trajectory must reach the switching plane M_3 at some positive time t_3, as shown in Fig. 7. Let $(-1, y_3, z_3, 0)$ be the hit point. According to the switching rule, this trajectory jumps onto Ω_3 holding y_3, z_3 constant. Thus, the hit point is $(-1, y_3, z_3, -1) \in \Omega_3$. Notice the symmetry of the vector field in both V_1 and V_{-1} Then, a trajectory started from $(-1, y_3, z_3, -1)$ in V_{-1} is symmetric to that started from $(1, -y_3, -z_3, 1)$ on Ω_1 in V_1. Now, one can define a two-dimensional Poincaré return map by

$$f : \Omega_1 \to \Omega_1,$$

$$(y_0, z_0) \to \begin{cases} (y_2, z_2) & \text{for } (y_0, z_0) \in H_0, \\ (-y_3, -z_3) & \text{for } (y_0, z_0) \in \bar{H}_0, \end{cases} \tag{21}$$

where $\bar{H}_0 = \Omega_1 - H_0$.

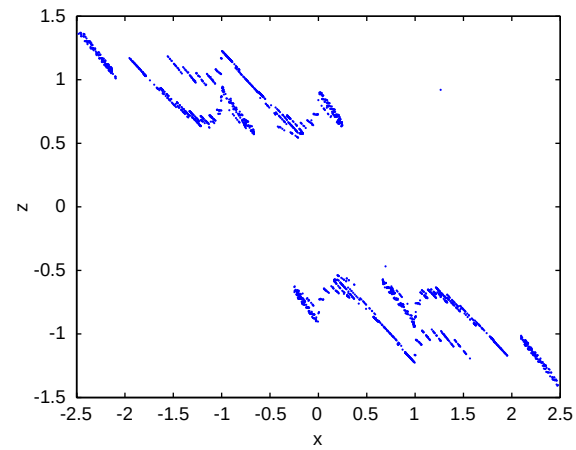

Fig. 8. Poincaré mapping at section $y = 0$ of the 3-scroll hysteresis system (7).

Clearly, one can get the rigorously mathematical formulation for this map by using the exact solution (18), as follows: (i) when $\bar{x}_0 = 0, \bar{y}_0 = y_0, \bar{z}_0 = z_0, t = t_1$, we get $\bar{x}(t_1) = -1, \bar{y}(t_1) = y_1, \bar{z}(t_1) = z_1$; (ii) when $\bar{x}_0 = 0, \bar{y}_0 = y_1, \bar{z}_0 = z_1, t = t_2 - t_1$, we have $\bar{x}(t_2 - t_1) = 1, \bar{y}(t_2 - t_1) = y_2, \bar{z}(t_2 - t_1) = z_2$; (iii) when $\bar{x}_0 = 0, \bar{y}_0 = y_1, \bar{z}_0 = z_1, t = t_3 - t_1$, we get $\bar{x}(t_3 - t_1) = -1, \bar{y}(t_3 - t_1) = y_3, \bar{z}(t_3 - t_1) = z_3$.

In actual calculations, one can use numerical methods, such as the Newton–Raphson method, to solve the equations. Moreover, the Jacobian matrix of this map f is described by

$$Df = \begin{cases} \begin{pmatrix} \dfrac{\partial y_2}{\partial y_0} & \dfrac{\partial y_2}{\partial z_0} \\ \dfrac{\partial z_2}{\partial y_0} & \dfrac{\partial z_2}{\partial z_0} \end{pmatrix} & \text{for} \quad (y_0, z_0) \in H_0 \\ -\begin{pmatrix} \dfrac{\partial y_3}{\partial y_0} & \dfrac{\partial y_3}{\partial z_0} \\ \dfrac{\partial z_3}{\partial y_0} & \dfrac{\partial z_3}{\partial z_0} \end{pmatrix} & \text{for} \quad (y_0, z_0) \in \bar{H}_0. \end{cases} \tag{22}$$

Remark 2. Now, one can calculate the Lyapunov exponents $\lambda_1, \lambda_2 (\lambda_1 \geqslant \lambda_2)$ of the Poincaré map f (Chen and Lü, 2003) by using the methods described in Lü et al. (2002a,b). In fact, one can get the exact mathematical formulations for λ_1, λ_2 from (22). However, the formulations are rather complex. In real calculations, one can use numerical methods discussed in Lü et al. (2002a,b) to calculate λ_1, λ_2. When $0 < \lambda_1 < +\infty$, system (7) with controller (8) is chaotic. Fig. 5 shows a 3-scroll hysteresis chaotic attractor, and its maximum Lyapunov exponent is $\lambda_1 = 0.0284 > 0$. Fig. 8 shows its Poincaré mapping at section $y = 0$.

Table 1
The detailed values for ζ, η, and A

i	j	ζ	η	A	Σ
1	1	0	y	$y \geqslant 0$	M_1
1	1	x	0	$x \geqslant 0$	N_1
0	1	1	y	$y \geqslant 0$	M_2
0	1	-1	y	$y \geqslant 0$	N_2
0	1	x	0	$-1 \leqslant x \leqslant 1$	P_2
-1	1	0	y	$y \geqslant 0$	M_3
-1	1	x	0	$x \leqslant 0$	N_3
1	0	0	y	$-1 \leqslant y \leqslant 1$	M_4
1	0	x	1	$x \geqslant 0$	N_4
1	0	x	-1	$x \geqslant 0$	P_4
0	0	1	y	$-1 \leqslant y \leqslant 1$	M_5
0	0	-1	y	$-1 \leqslant y \leqslant 1$	N_5
0	0	x	1	$-1 \leqslant x \leqslant 1$	P_5
0	0	x	-1	$-1 \leqslant x \leqslant 1$	Q_5
-1	0	0	y	$-1 \leqslant y \leqslant 1$	M_6
-1	0	x	1	$x \leqslant 0$	N_6
-1	0	x	-1	$x \leqslant 0$	P_6
1	-1	0	y	$y \leqslant 0$	M_7
1	-1	x	0	$x \geqslant 0$	N_7
0	-1	1	y	$y \leqslant 0$	M_8
0	-1	-1	y	$y \leqslant 0$	N_8
0	-1	x	0	$-1 \leqslant x \leqslant 1$	P_8
-1	-1	0	y	$y \leqslant 0$	M_9
-1	-1	x	0	$x \leqslant 0$	M_9

4.2. Hysteresis switching dynamics of system (7) with controller (11)

This subsection briefly discusses the hysteresis switching dynamics of system (7) with controller (11). Suppose that $p_1 = q_1 = p_2 = q_2 = 1$. Then system (7) with controller (11) has a 3×3-grid scroll chaotic attractor, which has nine equilibria, located in nine corresponding subspaces:

$$(i, j, 0, i, j) \in V_{(i,j)} \quad \text{for } -1 \leqslant i, j \leqslant 1$$

where $V_{(i,j)}(-1 \leqslant i, j \leqslant 1)$ are defined by (13). Note that system (7) with controller (11) has a natural symmetry under the coordinates transform $(x, y, z) \to (-x, -y, -z)$, which persists for all values of the system parameters.

Similarly, one can get the exact solution (18) of the hysteresis controlled system (7) with controller (11), where

$$(\bar{x}, \bar{y}, \bar{z})^{\mathrm{T}} = (x - i, y - j, z)^{\mathrm{T}} \quad \text{for } \bar{X} \in V_{(i,j)},$$

in which $\bar{X} = (x, y, z, u, v)$ and $-1 \leqslant i, j \leqslant 1$. Define the switching planes of the nine subspaces, $V_{(i,j)}(-1 \leqslant i, j \leqslant 1)$, as follows:

$$V_{(i,j)} : \Sigma \equiv \{(\zeta, \eta, z, i, j) | A\},$$

where ζ, η, and A are listed in Table 1.

Thus, the switching rules are obtained as

$$\begin{aligned}
V_{(1,1)} \quad &: \quad \bar{X}(t^+) \in V_{(0,1)} \cap \{x = 0\} \text{ if } \bar{X}(t) \in M_1, \\
& \quad \bar{X}(t^+) \in V_{(-1,1)} \cap \{y = 0\} \text{ if } \bar{X}(t) \in N_1; \\
V_{(0,1)} \quad &: \quad \bar{X}(t^+) \in V_{(1,1)} \cap \{x = 1\} \text{ if } \bar{X}(t) \in M_2, \\
& \quad \bar{X}(t^+) \in V_{(-1,1)} \cap \{x = -1\} \text{ if } \bar{X}(t) \in N_2, \\
& \quad \bar{X}(t^+) \in V_{(0,0)} \cap \{y = 0\} \text{ if } \bar{X}(t) \in P_2; \\
V_{(-1,1)} \quad &: \quad \bar{X}(t^+) \in V_{(0,1)} \cap \{x = 0\} \text{ if } \bar{X}(t) \in M_3, \\
& \quad \bar{X}(t^+) \in V_{(-1,0)} \cap \{y = 0\} \text{ if } \bar{X}(t) \in N_3; \\
V_{(1,0)} \quad &: \quad \bar{X}(t^+) \in V_{(0,0)} \cap \{x = 0\} \text{ if } \bar{X}(t) \in M_4, \\
& \quad \bar{X}(t^+) \in V_{(1,1)} \cap \{y = 1\} \text{ if } \bar{X}(t) \in N_4, \\
& \quad \bar{X}(t^+) \in V_{(0,-1)} \cap \{y = -1\} \text{ if } \bar{X}(t) \in P_4; \\
V_{(0,0)} \quad &: \quad \bar{X}(t^+) \in V_{(1,0)} \cap \{x = 1\} \text{ if } \bar{X}(t) \in M_5, \\
& \quad \bar{X}(t^+) \in V_{(-1,0)} \cap \{x = -1\} \text{ if } \bar{X}(t) \in N_5, \\
& \quad \bar{X}(t^+) \in V_{(0,1)} \cap \{y = 1\} \text{ if } \bar{X}(t) \in P_5, \\
& \quad \bar{X}(t^+) \in V_{(0,-1)} \cap \{y = -1\} \text{ if } \bar{X}(t) \in Q_5; \\
V_{(-1,0)} \quad &: \quad \bar{X}(t^+) \in V_{(0,0)} \cap \{x = 0\} \text{ if } \bar{X}(t) \in M_6, \\
& \quad \bar{X}(t^+) \in V_{(-1,1)} \cap \{y = 1\} \text{ if } \bar{X}(t) \in N_6, \\
& \quad \bar{X}(t^+) \in V_{(-1,-1)} \cap \{y = -1\} \text{ if } \bar{X}(t) \in P_6; \\
V_{(1,-1)} \quad &: \quad \bar{X}(t^+) \in V_{(0,-1)} \cap \{x = 0\} \text{ if } \bar{X}(t) \in M_7, \\
& \quad \bar{X}(t^+) \in V_{(1,0)} \cap \{y = 0\} \text{ if } \bar{X}(t) \in N_7; \\
V_{(0,-1)} \quad &: \quad \bar{X}(t^+) \in V_{(1,-1)} \cap \{x = 1\} \text{ if } \bar{X}(t) \in M_8, \\
& \quad \bar{X}(t^+) \in V_{(-1,-1)} \cap \{x = -1\} \text{ if } \bar{X}(t) \in N_8, \\
& \quad \bar{X}(t^+) \in V_{(0,0)} \cap \{y = 0\} \text{ if } \bar{X}(t) \in P_8; \\
V_{(-1,-1)} \quad &: \quad \bar{X}(t^+) \in V_{(0,-1)} \cap \{x = 0\} \text{ if } \bar{X}(t) \in M_9, \\
& \quad \bar{X}(t^+) \in V_{(-1,0)} \cap \{y = 0\} \text{ if } \bar{X}(t) \in N_9,
\end{aligned}$$

where $\bar{X} = (x, y, z, u, v)$, holding x, y, z constant during the switching.

Similarly, one can derive a condition for chaos generation with an $n \times m$-grid scroll attractor by constructing a two-dimensional Poincaré return map.

4.3. Hysteresis switching dynamics of system (7) with controller (14)

In this subsection, the hysteresis switching dynamics of system (7) with controller (14) are briefly discussed. Assume that $p_1 = q_1 = p_2 = q_2 = p_3 = q_3 = 1$. Then system (7) with controller (14) has a $3 \times 3 \times 3$-grid scroll chaotic attractor, which has 27 equilibria, located in 27 corresponding subspaces:

$$(i, j, k, i, j, k) \in V_{(i,j,k)} \quad \text{for } -1 \leqslant i, j, k \leqslant 1,$$

where $V_{(i,j,k)}(-1 \leqslant i,j,k \leqslant 1)$ are defined in Section 3.3. Obviously, system (7) with controller (14) has a natural symmetry under the coordinates transform $(x,y,z) \to (-x,-y,-z)$, which persists for all values of the system parameters.

It is easily to get the exact solution (18) of the hysteresis system (7) with controller (14), where

$$(X,Y,Z)^{\mathrm{T}} = (x-i, y-j, z-k)^{\mathrm{T}} \quad \text{for } \bar{X} \in V_{(i,j,k)},$$

in which $\bar{X} = (x,y,z,u,v,w)$ and $-1 \leqslant i,j,k \leqslant 1$.

Similarly, one can define the switching planes and switching rules for the hysteresis system (7) with controller (14). Also, a two-dimensional Poincaré return map can be derived to prove the chaotic behaviors for system (7) with controller (14) with an $n \times m \times l$-grid scroll attractor. However, the process is similar but rather complex, and hence its omitted here.

5. Conclusions

In this paper, we have introduced a systematic method for generating multi-scroll chaotic attractors, including 1-D n-scroll, 2-D $n \times m$-grid scroll, and 3-D $n \times m \times l$-grid scroll attractors, from a three-dimensional linear autonomous system with hysteresis series switchings. The hysteresis switching dynamics and chaos generation mechanism have also been investigated by analyzing the system trajectories. In particular, a two-dimensional Poincaré return map is rigorously derived for verifying the chaotic behaviors of the generated multi-scroll attractors. It is foreseeable that the hysteresis-series multi-scroll systems studied here will have wide applications in real-world engineering, where they can be used as novel chaotic generators.

Note that one can obtain a desired number of scrolls and their spatial positions and orientations using the developed methodology for some intended engineering applications. Future research will be conducted along the line of designing physical electronic circuit to verify experimentally the multi-scroll chaotic attractors (Cafagna & Grassi, 2003). On the other hand, understanding the hysteresis switching dynamics and the relative bifurcation analysis also deserve further investigation in the near future.

Finally, it should be noted that our theoretical analysis method developed here is generic and can be extended to the studies of k-D ($k \geqslant 3$) multi-scroll chaotic systems ($n \geqslant 3$). For example, lower-dimensional Poincaré return maps for higher-dimensional multi-scroll chaotic systems ($n \geqslant 3$) may be similarly constructed and their Lyapunov exponents can also be calculated. For visualization of multi-scroll attractors ($n \geqslant 3$), we may also observe various projections on 2-D planes and 3-D subspaces for k-D ($k \geqslant 3$) multi-scroll attractors.

Acknowledgements

This work was supported by the Hong Kong Research Grants Council under the CERG grant City U 1115/03E and the National Natural Science Foundation of China under Grant No. 60304017 and Grant No. 20336040/B06.

References

Cafagna, D., & Grassi, G. (2003). New 3D-scroll attractors in hyperchaotic Chua's circuit forming a ring. *International Journal of Bifurcation and Chaos*, *13*(10), 2889–2903.

Chen, G. (Ed.) (1999). *Controlling chaos and bifurcations in engineering systems*. Boca Raton: CRC Press.

Chen, G., & Dong, X. (1998). *From chaos to order: Methodologies, perspectives and applications*. Singapore: World Scientific.

Chen, G., & Lü, J. (2003). *Dynamics of the Lorenz system family: Analysis, control and synchronization*. Beijing: Science Press (in Chinese).

Elwakil, A. S., & Kennedy, M. P. (2000). Systematic realization of a class of hysteresis chaotic oscillators. *International Journal of Circuit Theory and Applications*, *28*(4), 319–334.

Elwakil, A. S., & Kennedy, M. P. (2001). Construction of classes of circuit-independent chaotic oscillators using passive-only nonlinear devices. *IEEE Transactions on Circuits and Systems, Part I*, *48*(3), 289–307.

Elwakil, A. S., Salama, K. N., & Kennedy, M. P. (2000). A system for chaos generation and its implementation in monolithic form. *Proceedings of the IEEE symposium on circuits and systems*, Geneva (pp. 217–220).

Han, F., Lü, J., Yu, X., Chen, G., & Feng, Y. (2004). A new systematic method for generating multi-scroll chaotic attractors from a linear second-order system with hysteresis. Accepted by Dynamics of Continuous, Discrete and Impulsive Systems, to appear.

Kataoka, M., & Saito, T. (2001). A two-port VCCS chaotic oscillator and quad screw attractor. *IEEE Transactions on Circuits and Systems, Part I*, *48*(2), 221–225.

Kennedy, A. S., & Kennedy, M. P. (1999). Chaotic oscillators derived from Saito's double-screw hysteresis oscillator. *IEICE Transactions on Fundamentals*, *E82*, 1769–1775.

Lü, J., Lu, J., & Chen, S. (2002a). *Chaotic time series analysis and its applications*. China: Wuhan University Press (in Chinese).

Lü, J., Zhou, T., Chen, G., & Yang, X. (2002b). Generating chaos with a switching piecewise-linear controller. *Chaos*, *12*(2), 344–349.

Lü, J., Yu, X., & Chen, G. (2003). Generating chaotic attractors with multiple merged basins of attraction: A switching piecewise-linear control approach. *IEEE Transactions on Circuits and Systems, Part I*, *50*(2), 198–207.

Nakagawa, S., & Saito, T. (1996). An RC OTA hysteresis chaos generator. *IEEE Transactions on Circuits and Systems, Part I*, *43*(12), 1019–1021.

Newcomb, R. W., & El-Leithy, N. (1986). Chaos generation using binary hysteresis. *Circuit System, Signal Processing*, *5*(3), 321–341.

Ozoguz, S., Elwakil, A. S., & Salama, K. N. (2002). *N*-scroll chaos generator using nonlinear transconductor. *Electronics Letters*, *38*(14), 685–686.

Saito, T. (1990). An approach toward higher dimensional hysteresis chaos generators. *IEEE Transactions on Circuits and Systems, Part I*, *37*(3), 399–409.

Saito, T., & Nakagawa, S. (1995). Chaos from a hysteresis and switched circuit. *Philosophical Transactions of The Royal Society of London Series A*, *353*, 47–57.

Storace, M., Parodi, M., & Robatto, D. (1999). A hysteresis-based chaotic circuit: Dynamics and applications. *International Journal of Circuit Theory and Applications*, *27*(6), 527–542.

Suykens, J. A. K., & Vandewalle, J. (1993). Generation of n-double scrolls ($n=1,2,3,4,\ldots$). *IEEE Transactions on Circuits and Systems, Part I*, *40*(11), 861–867.

Tang, K. S., Zhong, G. Q., Chen, G., & Man, K. F. (2001). Generation of n-scroll attractors via sine function. *IEEE Transactions on Circuits and Systems, Part I*, *48*(11), 1369–1372.

Yalcin, M. E., Ozoguz, S., Suykens, J. A. K., & Vandewalle, J. (2001). N-scroll chaos generators: a simple circuit model. *Electronics Letters*, *37*(3), 147–148.

Yalcin, M. E., Suykens, J. A. K., Vandewalle, J., & Ozoguz, S. (2002). Families of scroll grid attractors. *International Journal of Bifurcation and Chaos*, *12*(1), 23–41.

Zhong, G. Q., Man, K. F., & Chen, G. (2002). A systematic approach to generating n-scroll attractors. *International Journal of Bifurcation and Chaos*, *12*(12), 2907–2915.

Jinhu Lü received the B.Sc. degree in mathematics, the M.Sc. degree in applied mathematics, and Ph.D. degree in applied mathematics, from Hubei Normal University, Hubei, China, Wuhan University, Wuhan, China, and the Chinese Academy of Sciences, Beijing, China, in 1997, 2000, and 2002, respectively.

From January to April of 2002, he was a Research Assistant, and from August to November of 2003, a Senior Research Associate at the Centre for Chaos Control and Synchronization, City University of Hong Kong, Hong Kong. From January to May 2003, he was a Visiting Research Fellow in the School of Electrical and Computer Engineering, Royal Melbourne Institute of Technology University, Melbourne, Australia. From June 2002 to February 2004, he was a Postdoctoral Research Fellow, and from March 2003, an Assistant Professor with the Institute of Systems Science, Academy of Mathematics and Systems Sciences, Chinese Academy of Sciences, Beijing, China. Currently, he is a Postdoctoral Fellow in the Department of Electrical and Computer Engineering, University of Calgary, Calgary, Canada. He is the author of two research monographs, more than 50 research journal papers published in the fields of control and synchronization of complex dynamical systems.

Dr. Lü received the Presidential Outstanding Research Award from the Chinese Academy of Sciences in 2002 and the Top 100 National Best PhD Theses Award from the office of Academic Degrees Comittee of the State Council and the Ministry of Education of China in 2004.

Fengling Han received B.S. degree from the Department of Control Engineering, Harbin Shipbuilding Engineering Institute, China, in 1984, and M.S. degree from the Department of Control Engineering, Harbin Institute of Technology, China, in 1987, respectively. From 1987 to 2001, she was lecturing in the Department of Electrical Engineering, Harbin Institute of Technology, China. From 2001 to 2002, she was a PhD candidate with the Central Queensland University (CQU). In 2002, she was a Visiting Scholar in City University of Hong Kong. Since 2002, she has been a PhD candidate (transferred from CQU) with School of Electrical and Computer Engineering, Royal Melbourne Institute of Technology, Australia.

Her current research interests are electric network theory, nonlinear dynamical systems, fault location of power systems, digital camera modelling and simulation. She has published over 40 journal and conference papers and completed 4 research projects, including fault location of power systems, the electronics and simulation of CCD digital camera, anti-control of chaos and its application and so on.

Xinghuo Yu received B.E. and M.E. from the University of Science and Technology of China in 1982 and 1984, respectively, and Ph.D. degree from South-East University, China in 1988. From 1987 to 1989, he was a Research Fellow with Chinese Academy of Sciences, Beijing China. From 1989 to 1991, he was a Postdoctoral Fellow with the University of Adelaide, Australia. From 1991 to 2002, he was with Central Queensland University (CQU), Australia, where, before he left, he was Professor of Intelligent Systems, and the Associate Dean (Research) of the Faculty of Informatics and Communication. Since March 2002, he has been with the Royal Melbourne Institute of Technology (RMIT), Australia, where he is now a full Professor and the Associate Dean Research & Innovation of Science, Engineering and Technology of RMIT. He has held Visiting Professor positions at City University of Hong Kong and Bogazici University (Turkey). He is a Guest Chair Professor of four Chinese universities. Professor Yu's research interests include discontinuous and nonlinear control, chaos and chaos control, soft computing and applications. He has published over 250 refereed articles in technical journals, books and conference proceedings. He has also co-edited seven research books. Prof. Yu has served as an Associate Editor of IEEE Trans Circuits and Systems Part I (2001–2003). He has been on the program committees of over fourty international and national conferences. He was the sole recipient of the 1995 CQU's Vice Chancellor's Award for Research. He is a Fellow of Institution of Engineers Australia. Professor Yu was made Professor Emeritus of CQU in recognition of his significant contributions.

Guanrong Chen received the M.Sc. degree in Computer Science from the Sun Yat-sen (Zhongshan) University, China, and the Ph.D. degree in Applied Mathematics from Texas A&M University, USA. Currently he is a Chair Professor and the Founding Director of the *Centre for Chaos Control and Synchronization* at the City University of Hong Kong. He is a Fellow of the IEEE for his fundamental contributions to the theory and applications of chaos control and bifurcation analysis.

Prof. Chen has (co)authored 15 research monographs and advanced textbooks, more than 300 SCI journal papers, and about 180 refereed conference papers, published since 1981 in the fields of nonlinear system: dynamics and controls. Among his publications are the research monographs and edited books entitled *Hopf Bifurcation Analysis: A Frequency Domain Approach* (World Scientific, 1996), *From Chaos to Order: Methodologies, Perspectives and Applications* (World Scientific, 1998), *Controlling Chaos and Bifurcations in Engineering Systems* (CRC Press, 1999), *Chaos in Circuits and Systems* (World Scientific, 2002), as well as *Chaos Control* and *Bifurcation Control* (Springer, 2003).

Prof. Chen served and is serving as Deputy Chief Editor, Advisory Editor, Features Editor, and Associate Editors for 8 international journals including the IEEE Transactions on Circuits and Systems, IEEE Transactions on Automatic Control, and the International Journal of Bifurcation and Chaos. He received the 1998 Harden-Simons Prize for the Outstanding Journal Paper Award from the American Society of Engineering Education and the 2001 M. Barry Carlton Best Annual Transactions Paper Award from the IEEE Aerospace and Electronic Systems Society. He is Honorary Professor of the Central Queensland University, Australia, as well as Honorary Guest-Chair Professor of more than ten Universities in China.